Proceedings of the 21st ICSMGE, Vienna, Austria, 14 – 19 June 2026. Pistrol, Adam & Schweiger (eds.)
Published by: ÖGG, Austrian Society for Geomechanics, Salzburg, Austria, ISBN 978-3-9503898-4-5
https://doi.org/10.53243/ICSMGE2026-354

Stability of Infinite Slopes in Low-Density Pyroclasts

Rubén Galindo, Noelia Esteban, Miguel Ángel Millán, Fausto Molina
Universidad Politécnica de Madrid, Madrid, Spain, rubenangel.galindo@upm.es

ABSTRACT: This work focuses on the theoretical and parametric analysis of the failure depth of infinite slopes in low-density pyroclastic rocks. Their undefined geometry allows the failure to be approximated as a shallow slide along a planar surface parallel to the slope inclination. Through a mathematical development based on static equilibrium and the application of the collapse criterion equations for this material, a general limit equilibrium expression for an infinite slope is derived. The resulting formulation accounts for the material's destructuring (mechanical collapse) and depends on the parameters of collapse pressure, rock tensile strength, and a frictional parameter. Additionally, a sensitivity analysis has been carried out with respect to slope inclination and the direction of water flow. The study results are presented in the form of charts (abaci), which allow estimation of the failure depth under different conditions of the analyzed slope.

KEYWORDS: Slope stability, pyroclasts, macroporous rocks, collapse, volcanic rocks, analytical solution

1 INTRODUCTION

The geotechnical analysis of slope failure has advanced significantly through the development of diverse theoretical and empirical models. This study contributes to the field by focusing on infinite slopes in macroporous volcanic rock masses, particularly low-density pyroclastic deposits characterized by high porosity and complex geomechanical behavior.

Instability often occurs in excavated slopes within volcanic terrains, posing risks to infrastructure and population due to landslides and rockfalls. These phenomena are especially critical along transportation networks and urban or recreational areas, which often require urgent mitigation measures (Michoud et al., 2012; Martino et al., 2014).

The concept of an infinite slope, defined as a mathematical simplification neglecting the effects of toe and crest, is especially suitable for analyzing shallow failures in these materials. However, conventional failure criteria prove inadequate when applied to low-density volcanic deposits, whose structural collapse under stress involves particle bond breakage and volumetric compaction, leading to non-linear and irreversible mechanical responses.

Experimental research on volcanic materials has highlighted this unique behavior (Pellegrino, 1970; Adachi et al., 1981; Moon, 1993; Aversa & Evangelista, 1998; Cecconi & Viggiani, 2001). At low stress levels, these materials may exhibit conventional strength parameters, yet, beyond a critical threshold, a collapse mechanism is activated, marked by a loss of structure and a transition to a denser particle arrangement.

This study adopts a failure criterion based on collapse mechanics failure developed by Serrano et al. (2016), grounded in previous research on low-density volcanic soils from regions such as the Canary Islands (Serrano et al., 2002). The criterion incorporates variables such as compaction, welding, particle strength, imbrication, and degree of alteration. This model is reformulated in parametric terms to align with infinite slope equilibrium equations, as previously outlined by Serrano et al. (2004), and applied to assess the potential for mechanical collapse of natural and excavated slopes.

In summary, the proposed approach integrates collapse mechanics into slope stability analysis for macroporous volcanic rocks, offering a more realistic representation of failure mechanisms in such materials. This contributes to improving the predictive capabilities of slope stability models and informs better design and hazard mitigation strategies in volcanic environments.

2 FORMULATION OF SLOPE STABILITY EQUILIBRIUM

2.1 *General Considerations*

The formulation developed by Serrano et al. (2004) for evaluating failure within infinite slopes using the Hoek-Brown criterion, and later extended by Esteban and Galindo (2022), aims to define the depth of the failure plane. A simplified summary adapted to the requirements of this study is presented below.

The mathematical formulation is based on the following assumptions: (1) the slope is infinite, and an analysis of infinitesimal slices is performed (Figure 1); (2) the material is homogeneous and isotropic; (3) no external forces are applied; (4) the stress and strain tensors are coaxial.

The formulation is non-dimensionalized to simplify the analytical expressions using the dry specific weight and stress parameters as follows: (1) the dry weight of the rock (γ_d^*); (2) the normalized collapse strength of the rock ($\beta^* = P_c^* + t^*$), where P_c^* is the isotropic compressive strength and t^* is the isotropic tensile strength.

This ensures that all relevant quantities in the problem are considered. In terms of notation, a parameter denoted as w^* has physical dimensions, whereas w denotes its dimensionless counterpart.

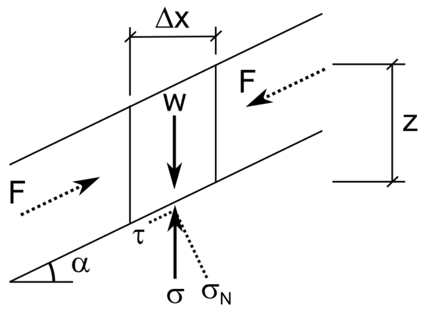

Figure 1. Equilibrium of a Slice of an Infinite Slope.

2.2 *Strength of the Failure Plane*

The strength of the failure surface is defined using a general failure criterion, which involves the instantaneous friction angle (ρ) and the dilatancy angle (ψ). The failure equations, expressed in terms of Lambe parameters (p', q), are given in Equation (1).

$$\tau = q \cdot \cos\psi ; \sigma_N = p' - q \cdot \sin\psi \quad (1)$$

Thus, the mobilized instantaneous friction angle at failure is defined by Equation (2).

$$\tan\rho = \frac{\tau}{\sigma_N} = \frac{q \cdot \cos\psi}{p' - q \cdot \sin\psi} \tag{2}$$

This formulation allows the failure criterion to be expressed as a function of the instantaneous friction angle, yielding a closed-form expression. To define the dilatancy angle, a general linear flow rule can be applied in Equation (3) (dependent on two parameters, a_1 and a_2; $a_1 = 0$ and $a_2 = 1$ corresponds to the associated flow case).

$$\sin\psi = a_1 + a_2 \cdot \sin\rho \tag{3}$$

2.3 *Considerations on Water Flow within the Slope Body*

A general groundwater flow within the slope is considered, flowing at an inclination defined by the angle i, which is generally not parallel to the slope surface. Figure 2 illustrates this hydraulic flow conditions, which generates a pore water pressure u, from which the variable $r_{u\alpha}$ is defined in Equation (4).

$$r_{u\alpha} = \frac{u}{\sigma_N} = \frac{\gamma_w^* \cos i}{\gamma_d^* \cos(i-\alpha)\cos\alpha} \tag{4}$$

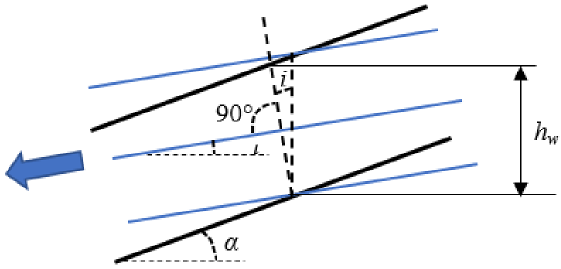

Figure 2. Diagram of the effect of water flow on a slope inclined at angle α.

An equivalent virtual slope, with inclination angle α_i, is defined as the slope that, in the absence of water, fails in the same manner as a slope of inclination α with a flow net inclined at angle i. This relationship is expressed in Equation (6).

$$\tan\alpha_i = \tan\alpha / (1 - r_{u\alpha}) \tag{6}$$

2.4 *Slope Stability Equations*

The failure plane depth of the slope is defined by the critical vertical depth H_{crit} (Equation (7)), or by the critical thickness d_{crit} parallel to the slope.

$$H_{crit} = \frac{\tau}{\cos\alpha \sin\alpha} = \frac{q \cdot \cos\psi}{\cos\alpha \sin\alpha} \tag{7}$$

To simplify the expressions and reduce the number of parameters, the final equations are expressed in terms of the virtual slope. For the virtual slope, the equilibrium condition (Equation 8), defined using the mobilized instantaneous friction angle (Equation 2), is satisfied. The failure depth (Equation 9) and the flow law (Equation 3) are also applied.

$$\tan\alpha_i = \tan\rho = \frac{q(\rho) \cdot \cos\psi}{p'(\rho) - q(\rho) \cdot \sin\psi} \tag{8}$$

$$d_{crit,i} = H_{crit,i} \cos\alpha_i = \frac{q(\rho) \cdot \cos\psi}{\sin\alpha_i} \tag{9}$$

As mentioned earlier, the formulation is developed using a non-dimensionalization approach. After obtaining results for thickness and failure depth, the variables are reverted according to Equations (10).

$$d_{crit,i}^* = d_{crit,i} \cdot \frac{\beta^*}{\gamma_d^*};\ H_{crit,i}^* = H_{crit,i} \cdot \frac{\beta^*}{\gamma_d^*} \tag{10}$$

3 PARAMETRIC FORMULATION OF THE COLLAPSE FAILURE CRITERION

3.1 *Failure Criterion*

The formulation by Serrano et al. (2004) for evaluating failure in infinite slopes using the Hoek-Brown criterion, and later extended by Esteban and Galindo (2022), aims to define the depth of the failure plane. A simplified summary, adapted to the requirements of this study, is presented below. The failure criterion equations for collapsible rocks are based on the empirical study conducted on volcanic pyroclasts by Serrano et al. (2016). In that study, a parabolic formulation was proposed as a strength criterion for low-density pyroclastic materials. Before this development, other authors (Pellegrino, 1970; Aversa and Evangelista, 1998) proposed different yield surfaces for low-density, collapsible materials, which motivated the empirical study and the parabolic criterion used here.

The study of low-density volcanic materials indicated that the geomechanical behavior of these materials is highly conditioned by their structure. At low confining stress levels, the stress–strain behavior can be considered elastic and linear; however, after reaching the peak stress, the material exhibits significant brittleness, which becomes more pronounced as confinement decreases.

The failure criterion for low-density pyroclasts, as proposed by Serrano et al. (2016), is expressed in Cambridge variables (p^*, q^*) as is indicated in (11).

$$q^* = M(p^* + t^*)\left(1 - \frac{p^* + t^*}{P_c^* + t^*}\right)^{\lambda} \tag{11}$$

In Equation (11), there are three parameters: t^* is the isotropic tensile strength, P_c^* is the isotropic compressive strength (or collapse pressure), and M is a frictional parameter that can be determined through triaxial testing at low stress levels, depending on the instantaneous friction angle (ρ_o). The parameter λ is an experimentally calibrated exponent.

Equation (11) uses dimensional parameters and variables, as indicated by the notation. The dimensionless reformulation of the collapse criterion and its reorganization into parametric expressions compatible with the infinite slope model are addressed in the following sections.

The parameters of the failure law were determined for various pyroclast types through triaxial tests under low-stress conditions. Conde (2013) found that welded lapilli have lower average values for the parameter t^* (9% of the collapse pressure on average) compared to pumice (average of 18%), with most pyroclasts showing much lower average values (around 1%). As for the parameter M, most materials were found to have values between 1.5 and 3. The exponent λ, on the other hand, takes a value very close to 1 in most volcanic lithotypes, thus, this value may be considered a reasonable approximation. However, the general expression will be developed for any value of λ.

This study provides an important basis for understanding the mechanical behavior of volcanic rock masses and for developing more accurate and reliable slope stability models in volcanic environments.

3.2 *General Principles of the Parametric Formulation*

The failure criterion for volcanic rocks comprises two distinct zones in the Cambridge stress diagram: one corresponding to stress paths prior to the critical collapse point (sliding failure), and the other corresponding to stress paths that end beyond the critical point (destructuring). Figure 3 shows a schematic representation of the failure surface using dimensionless Cambridge variables $(p = (p^* + t^*)/(P^*{}_c + t^*); q = q^*/(P^*{}_c + t^*))$.

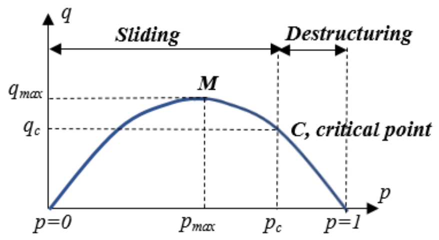

Figure 3. General scheme of the failure criterion for collapsible rocks in dimensionless Cambridge variables.

Each of the two branches of the failure criterion is defined by an expression in Cambridge variables. These expressions must be rewritten in parametric form to be incorporated into the system of equations used to determine the failure depth of the infinite slope. The formulations presented in the following sections have been non-dimensionalized according to the criterion introduced in Section 2.1. This approach applies to all equations in this section.

3.3 *Failure Formulation for λ = 1*

The failure criterion, expressed in Lambe variables, is given in Equation (12).

$$q = 3 \cdot \left(-\kappa + p + \sqrt{\kappa^2 - 2ap}\right) \tag{12}$$

The auxiliary variables κ and a depend on the frictional parameter M, as defined in Equation (13).

$$\kappa = \frac{M+6}{2M};\ a = \frac{3}{M} \tag{13}$$

The Equation (14) between the failure criterion and the instantaneous friction angle (ρ), which is the main variable in the slope analysis, is established by its definition as the ratio between the differentials of p and q.

$$\sin\rho = \frac{dq}{dp} = 3\left(1 + \frac{a}{\sqrt{\kappa^2 - 2ap}}\right) \tag{14}$$

At the critical collapse point (point C, Figure 3), the differential of the expression takes the following value:

$$\sin\rho = \frac{dq}{dp} = -1 \tag{15}$$

This yields the corresponding value of p at the critical transition point:

$$p_C = \frac{(2M+3)(2M+21)}{96M} \tag{16}$$

This expression is relevant for determining which branch the failure point associated with a given slope belongs to. Assuming an associated flow rule, the dilatancy angle ψ equals the friction angle ρ.

$$\begin{aligned} p \le p_C &\rightarrow |\sin\psi| = |\sin\rho| \le 1 \rightarrow \textit{slide} \\ p > p_C &\rightarrow |\sin\psi| = |\sin\rho| > 1 \rightarrow \textit{collapse} \end{aligned} \tag{17}$$

The parametric expression of the failure criterion can be expressed as a function of the instantaneous friction angle (ρ), which is expressed in terms of the auxiliary variable s.

$$s = 1 - \frac{1}{3} \cdot \sin\rho \tag{18}$$

$$p = \frac{(M+6)^2}{24M} - \frac{3}{2M \cdot s^2} \tag{19}$$

$$q = \frac{1}{8M \cdot s^2}[(M-6) \cdot s + 6] \cdot [(M+6) \cdot s - 6] \tag{20}$$

Substituting the variable s and rearranging the expressions yields the parametric equations used to solve the slope failure system.

$$p = \frac{(M+6)^2}{24M} - \frac{27}{2M \cdot (3 - \sin\rho)^2} \tag{21}$$

$$q = \frac{36 - M^2}{8M} \cdot \frac{(b - \sin\rho)(c + \sin\rho)}{(3 - \sin\rho)} \tag{22}$$

Where $b = \frac{3M}{6+M}$ and $c = \frac{3M}{6-M}$.

3.4 *Complete System of Equations*

Once the expressions for slope failure and the parametric equations of the failure criterion are established, the complete dimensionless equations is given below.

Failure of the infinite slope: Equations (8) and (9)

Associated flow rule: $\psi = \rho$

Verification equation of the branch of the failure criterion: Equation (17)

Parametric equations of failure: Equations (21) and (22)

In both cases, the complexity of the resulting single mathematical expression requires the use of approximate numerical methods. Specifically, a Newton-Raphson iterative method for non-linear equation solving is used to estimate the calculation variable ρ.

The resolution of the system of equations depends on the primary variable. If the failure point lies on the sliding branch, the system is solved directly in terms of the instantaneous friction angle (ρ). For the destructuring branch, the system is first solved in terms of the variable f, which allows derivation of p, q, and ρ.

4 RESULTS AND DISCUSSION

The obtained formulations have been implemented using spreadsheets and organized in the form of charts. The graphs below illustrate the evolution of the failure thickness of the infinite slope as a function of the equivalent slope angle, which depends on the slope inclination and the hydraulic flow direction through the use of the virtual slope, according to the criteria summarized in Section 2.3. The evolution of the critical failure thickness is presented on a logarithmic scale to improve the clarity of the charts.

The graphs developed within this study include a failure thickness line calculated for different values of the rock friction parameter M. Three values (M = 1.5, 2.0, 2.5) have been selected within the typical range to study their direct influence on the failure depth. Simultaneously, a sensitivity analysis of the critical failure depths was performed based on variations in the isotropic collapse strength parameter, assuming reasonable values (P_c^*=1.0, 2.0, 4.0 MPa). For the calculations, a dry unit weight of the rock (γ_d^*= 16 kN/m^3) and an isotropic tensile strength equal to 10% of the collapse strength were assumed.

The results of this analysis are presented in Figure 4. The results indicate that the failure depth decreases significantly as the slope angle increases, reflecting that planar failures are more likely because they involve a smaller displaced mass of soil at steeper inclinations. The decrease in failure thickness evolves gradually, although it tends to stabilize for high equivalent slope angles, from 60 to 80°.

Regarding the magnitude of the mobilized thickness, a range of 2 to 3 orders of magnitude in failure thickness along the failure surface is observed, depending on the slope angle. For low slope angles, the high failure thickness corresponds to a low or even negligible probability of mobilization. An important observation from the graphs is that, while the absolute magnitude of the failure thickness varies somewhat depending on the rock mass characterization parameters, the range of reduction with respect to slope inclination remains consistent.

Concerning the influence of the friction parameter M, all the graphs show that higher values result in greater failure thicknesses, with differences that can reach up to one order of magnitude in the region of greatest variation of the resulting critical thickness.

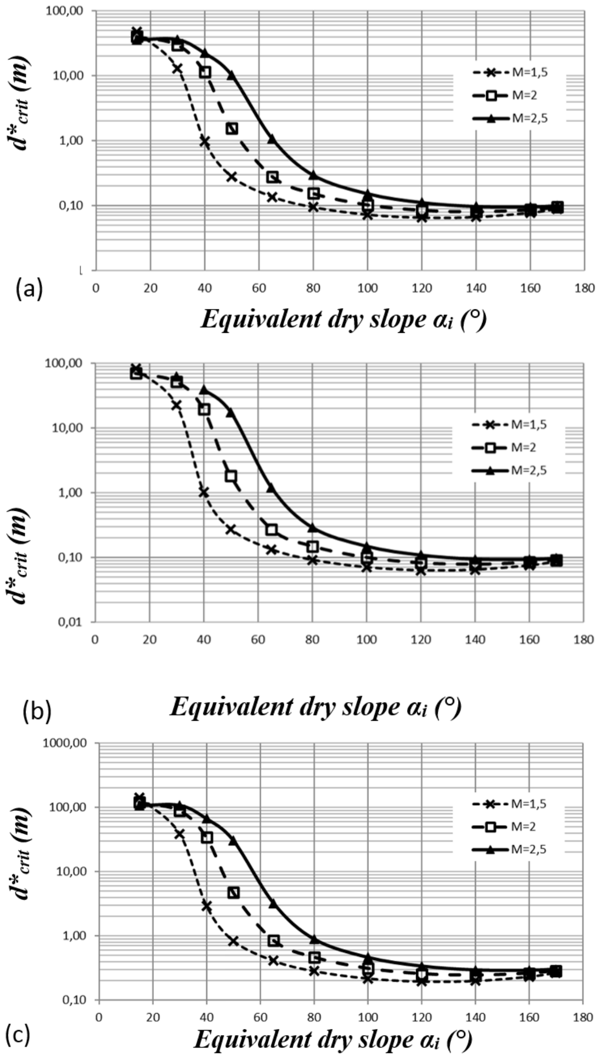

Figure 4. Failure thickness with associated flow rule, as a function of slope inclination and water flow, for a rock mass with parameter β^*: (a) 1.1 MPa; (b) 2.2 MPa; (c) 4.4 MPa.

5 CONCLUSION

A mathematical model has been developed to estimate the failure depth in infinite slopes composed of macroporous pyroclastic rock, modeled as a collapsible material.

A tool has been implemented to generate charts (abaci) that show the evolution of failure thickness in infinite slopes of collapsible pyroclastic rock, as a function of slope inclination and hydraulic flow conditions.

The results show that slopes with inclinations below 20–30° exhibit failure thicknesses associated with a low probability of failure. Above these values, the critical thickness decreases rapidly, depending on the characteristics of the pyroclastic rock mass.

The derived formulation exhibits reasonable sensitivity to variations in rock mass quality parameters, primarily the isotropic compressive strength.

6 ACKNOWLEDGEMENTS

This publication is part of the project PID2022-139202OB-I00, *Neural networks and optimization techniques for the safe design and maintenance of transport infrastructure: geotechnics of volcanic rocks and slope stability (IA-Pyroslope)*, funded by the State Research Agency of the Ministry of Science, Innovation and Universities and the European Regional Development Fund, MCIN/AEI/10.13039/501100011033/FEDER, EU.

7 REFERENCES

Adachi, T., Ogawa, T., and Hayashi, M. 1981. Mechanical properties of soft rock and rock mass. *Proc. 10th ICSMFE 1*: 527-530.

Aversa, S., and Evangelista, A. 1998. The mechanical behavior of a pyroclastic rock: failure strength and "destruction" effects. *Rock mechanics and Rock Engineering,* 31, 25-42 (1998).

Cecconi, M., and Viggiani, G. 2001. Physical and structural properties of a pyroclastic soft rock. The Geotechnics of Hard Soils-Soft Rocks. *2do International Symposium on Hard Soils-Soft Rocks*, Naples, Italy, 1: 85-91.

Conde, M. 2013. *Caracterización Geotécnica de Materiales Volcánicos de baja Densidad*. Ph.D. Thesis, Universidad Complutense de Madrid, Madrid, Spain.

Esteban, N., and Galindo, R. 2022. Estudio de la profundidad de rotura de taludes indefinidos en macizos rocosos. *XI Symposio Nacional de Ingeniería Geotécnica*, Mieres, España, ISSN: 978-84-09-40096-6.

Martino, S., and Mazzanti, P. 2014. Integrating geomechanical surveys and remote sensing for sea cliff slope stability analysis: the Mt. Pucci case study (Italy), *Nat. Hazards Earth Syst. Sci.*, 14: 831–848, https://doi.org/10.5194/nhess-14-831-2014.

Michoud, C., Derron, M.-H., Horton, P., Jaboyedoff, M., Baillifard, F.-J., Loye, A., Nicolet, P., Pedrazzini, A., and Queyrel, A. 2012. Rockfall hazard and risk assessments along roads at a regional scale: example in Swiss Alps, *Nat. Hazards Earth Syst. Sci.*, 12: 615–629, https://doi.org/10.5194/nhess-12-615-2012

Moon, V.G. 1993. Geotechnical characteristics of ignimbrite: a soft pyroclastic rock type. *Eng. Geology* 5(1–2): 33-48.

Pellegrino, A. 1970. Mechanical behaviour of soft rocks under high stresses. *ISRM, II Congreso Internacional de Mecánica de Rocas*, Tomo II, Belgrado, R, 3, 25.

Serrano, A., Olalla, C., and Manzanas, J. 2004. *Estabilidad de taludes rocosos infinitos con criterios de rotura no lineales y leyes de fluencia no asociadas*. Editorial: Centro de Estudios y Experimentación de Obras Públicas.

Serrano, A., Olalla, C., and Perucho, A. 2002. Mechanical collapsible rocks. *Proceedings of the 1st Workshop on Volcanic Rocks*, Eurock, Funchal, 105–113.

Serrano, A., Perucho, A., and Conde, M. 2016. Yield criterion for low-density volcanic pyroclasts, *International Journal of Rock Mechanics and Mining Sciences*, Volume 86: 194-203, https://doi.org/10.1016/j.ijrmms.2016.04.014.